Received: 11 February 2020 | Revised: 27 April 2020 | Accepted: 12 May 2020

DOI: 10.1002/pip.3298

SHORT COMMUNICATION

PROGRESS IN PHOTOVOLTAICS WILEY

Impact of bilayer structures on the surface passivation quality of high-rate-sputtered hydrogenated amorphous silicon for silicon heterojunction solar cells

Faris Akira Bin Mohd Zulkifly | Yuta Shiratori | Kazuyoshi Nakada | Shinsuke Miyajima

Department of Electrical and Electronic Engineering, Tokyo Institute of Technology, Meguro-ku, Tokyo, 152-8550, Japan

Correspondence
Shinsuke Miyajima, Department of Electrical and Electronic Engineering, Tokyo Institute of Technology, Meguro-ku, Tokyo 152-8550, Japan.
Email: miyajima.s.aa@m.titech.ac.jp

Funding information
New Energy and Industrial Technology Development Organization, Grant/Award Number: 15100647-0

Abstract

Crystalline silicon surface passivation effect of intrinsic hydrogenated amorphous silicon (i-a-Si:H) films deposited by radio-frequency facing target sputtering (RF-FTS) using a two-step deposition technique was investigated. In the two-step deposition technique, an i-a-Si:H layer was deposited at a high sputtering power condition after the deposition of i-a-Si:H at a low sputtering power condition. The two-step deposition technique drastically improved the passivation quality of i-a-Si:H compared with a conventional single-step deposition technique. Only 0.5-nm-thick i-a-Si:H deposited at a low sputtering power suppresses the initial sputtering damage to the crystalline silicon surface. A high average deposition rate of 14.1 nm/min was also achieved. A non-textured silicon heterojunction solar cell using an i-a-Si:H passivation layer deposited by the two-step method shows a conversion efficiency of 17.4% (V_{oc} = 0.679 V, J_{sc} = 35.0 mA/cm^2, *FF* = 0.732).

1 | INTRODUCTION

Crystalline silicon solar cell technology continues to be the dominant solar cell production route for photovoltaic power generation systems. The passivated emitter and rear cell (PERC) type silicon solar cell[1–3] is gradually replacing the conventional aluminum back surface field (Al-BSF) type solar cell because of its higher efficiency. For further improvement of conversion efficiency, silicon heterojunction (SHJ) solar cells are promising candidates.[4–6]The key point of the SHJ solar cell structure is the application of a surface passivation technology using intrinsic hydrogenated amorphous silicon (i-a-Si:H), which reduces the surface recombination at the interface of the crystalline silicon wafer.[7–9] As the conversion efficiency continues to approach the theoretical limits, the development of a low-cost fabrication technology is gaining more attention in recent years.[10]

Recently, our group has been working on the application of intrinsic hydrogenated amorphous silicon deposited by radio frequency facing target sputtering (RF-FTS)[11–14] as an alternative approach to replace the standard plasma-enhanced chemical vapor deposition (PECVD) and catalytic chemical vapor deposition (Cat-CVD).[15–19] The main benefits of FTS are the non-use of hazardous SiH_4 gas during the film deposition process, small sputtering damage, and high deposition rate compared with conventional magnetron sputtering.[20,21] In our previous work, we demonstrated good surface passivation quality of relatively thick i-a-Si:H (45 nm) deposited by RF-FTS.[22] A crystalline silicon wafer passivated by 45-nm-thick i-a-Si:H shows a minority carrier lifetime of 2 ms at a minority carrier density of 10^{15} cm^{-3} and an implied open circuit voltage (iV_{oc}) of 0.719 V at one sun. In addition, the effect of RF power on the properties of i-a-Si:H films was also analyzed. Although high RF power improved the electrical properties of the i-a-Si:H film, the increased sputtering damage toward the c-Si surface limited the surface passivation quality. In our very recent work, we found that DC-superimposed RF-FTS improved the deposition rate of i-a-Si:H (6.8 nm/min) without deterioration of surface passivation quality.[23] However, the surface passivation quality for a thin i-a-Si:H layer (~6 nm) was still low. Improving the surface passivation quality of thin i-a-Si:H is necessary for its application in SHJ solar cells.

Faris Akira Bin Mohd Zulkifly and Yuta Shiratori contributed equally to this work.

To improve the passivation quality of thin i-a-Si:H deposited by DC-superimposed RF-FTS, it is important to deposit high quality i-a-Si:H at the initial stage of the deposition. As mentioned above, high quality i-a-Si:H can be deposited at high RF-power condition, however, the c-Si surface receives large sputtering damage under the high RF-power condition. One of the ideas to suppress the sputtering damage is inserting a very thin i-a-Si:H layer deposited at low RF-power between the c-Si and the i-a-Si:H layer deposited at high RF-power. This deposition method is referred to as two-step deposition technique. A bilayer structure has also been used in the deposition process of PECVD i-a-Si:H passivation layers. The combination of the deposition conditions of each layer affects the passivation quality of i-a-Si:H.[9] Therefore, it is important to investigate the effect of deposition conditions of both layers in the bilayer structure. In this paper, we report the effect of first and second i-a-Si:H layers on the passivation quality of relatively thin (∼6 nm) i-a-Si:H bilayer deposited by DC-superimposed RF-FTS.

2 | EXPERIMENTAL METHODS

Float-zone double-side-polished n-type monocrystalline silicon (100) wafers with a thickness of 280 μm and resistivity of 1–5 Ω·cm were used in this study. After cutting the wafers into small pieces (7 cm square), the as-cut Si wafer was dipped in a diluted 1% hydrofluoric acid solution for 60 s to remove the native oxide on the wafer surface. Subsequently, bilayer stacked i-a-Si:H layers were sputtered symmetrically on both sides of the cleaned silicon wafer by using a FTS system (FTS Corporation, NFTS-3S-DI-001) at room temperature. The sample structure is shown in Figure 1. In this study, DC-superimposed RF-FTS is used for the film deposition. In the DC-superimposed RF-FTS, both RF (13.56 MHz) and DC power were supplied to the FTS system simultaneously. Details of each power source condition used in this study are described below. The silicon targets used in this study were two phosphorous-doped monocrystalline silicon targets with a resistivity ranging from 57 to 75 Ω·cm. The sputtering gas was a mixture of Ar: 95% and H_2: 5%, and sputtering pressure was fixed at 0.2 Pa.

There were three main experiments for the optimizations of the bilayer stacked i-a-Si:H deposited by using the two-step deposition method. The total thickness of the i-a-Si:H layer for each experiment was kept constant at 6 nm. For the optimizations, the supplied DC-power was fixed at 25 W. The effects of RF-power for the second i-a-Si:H deposition, RF-power for the first i-a-Si:H deposition, and the thicknesses of both i-a-Si:H layers were investigated. The parameters used for each experiment are summarized in Table 1. For the first experiment, the deposition condition of the first i-a-Si:H layer was fixed (RF 300 W, 1 nm), whereas for the 5-nm-thick second i-a-Si:H layer, the RF power was varied in the range of 300–600 W. For the second experiment, the deposition condition of the second i-a-Si:H layer was fixed (RF 600 W, 5 nm), whereas for the 1-nm-thick first i-a-Si:H layer, the RF power was varied in the range of 200–600 W. For the third experiment, the RF power of the first and second i-a-Si:H layers were fixed at 300 and 600 W, respectively. The thicknesses of each of the two layers were varied while keeping the total thickness to 6 nm.

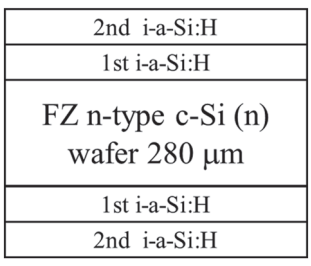

FIGURE 1 The structure of the samples used to investigate the passivation quality of i-a-Si:H deposited by using two-step deposition method. The second layer was deposited without turning off the plasma of the facing target sputtering (FTS) system

The thicknesses were controlled by setting the sputtering time based on the deposition rate shown in Figure 2. Both i-a-Si:H layers were deposited continuously without stopping the plasma. After the deposition of the i-a-Si:H film, a post-deposition annealing treatment was carried out for each sample in forming gas ambient (N_2: 97%, H_2: 3%) with the temperature in the range of 250°C–400°C for 1 min. Spectroscopic ellipsometry (SE) and quasi-steady-state-photoconductance (QSSPC) were used for the characterization of the samples. It is very difficult to measure the thickness and optical properties of each layer using SE because both first and second layers have similar optical properties. The total thickness and optical properties of the i-a-Si:H layer were therefore measured as a single layer using Tauc–Lorentz model.[24]

After optimization of the bilayer thicknesses, we compared the passivation quality of i-a-Si:H deposited by two-step and one-step deposition methods. For this comparison, the applied DC power was slightly changed from 25 to 56 W because we recently found that better passivation quality and higher deposition rate is expected by using the DC power of 56 W.[25] We also fabricated a SHJ solar cell with this i-a-Si:H layer to show the potential of sputtered i-a-Si:H. The structure of the solar cell was LiF anti-reflection coating (65 nm)/Al/Ag/ITO/p-type hydrogenated microcrystalline silicon oxide (20 nm)/i-a-Si:H (4.5 nm)/n-type c-Si (280 μm)/i-a-Si:H (2.5 nm)/n-type hydrogenated microcrystalline silicon (30 nm)/ITO/Ag/Al. The n-type c-Si wafer was not textured. The p-type and n-type

TABLE 1 Key parameters used in the three different experiments

Parameter	First experiment	Second experiment	Third experiment
RF power for the first layer (W)	300	200–600	300
RF power for the second layer (W)	300–600	600	600
Thickness for the first layer (nm)	1	1	0–6
Thickness for the second layer (nm)	5	5	6–0

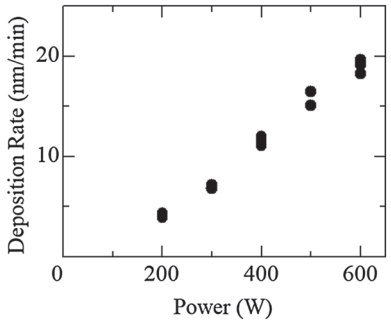

FIGURE 2 Dependence of the deposition rate of i-a-Si:H on radio frequency (RF) power. The DC power was fixed at 25 W. The deposition rate was calculated from the thickness of the deposited i-a-Si:H (thickness < 7 nm) and sputtering time. The deposition rate linearly increased with increasing the RF power and relatively high deposition rate was obtained at high RF power

microcrystalline silicon-based layers were deposited by PECVD. The p-type layer was deposited by VHF-PECVD with a frequency of 60 MHz. The flow rates of SiH_4, H_2, CO_2, and B_2H_6 were 2.5, 261, 0.4, and 0.003 sccm, respectively. The process pressure and VHF-power-density were 100 Pa and 0.25 W/cm^2. The n-type layer was deposited by RF-PECVD. The flow rates of SiH_4, H_2, and PH_3 were 3.0, 302, and 0.016 sccm. The process pressure and RF-power were 200 Pa and 0.13 W/cm^2. The substrate temperature was 170°C for both depositions. Before depositing the ITO layers, thermal annealing at 225°C in forming gas ambient was carried out to enhance the surface passivation quality. The ITO layer was deposited by RF-magnetron sputtering using an ITO target (SnO_2:In_2O_3 = 1:9). The sputtering gas was pure Ar at the pressure of 0.5 Pa. The RF power for the sputtering was 1.0 W/cm^2. The distance between the ITO target and the solar cell substrate was 10 cm. The Al/Ag electrodes and LiF anti-reflection coating were deposited by thermal evaporation. Thicknesses of the rear Ag/Al electrode were 500 nm/2500 nm. The thicknesses of the front Ag/Al electrode were 500 nm/9000 nm. The finished solar cell was annealed at 200°C in N_2 for 5 min.

3 | RESULTS

Figure 3 shows the effect of the RF power for the second i-a-Si:H deposition on optical bandgap and effective lifetime. The optical bandgap decreased with increasing the RF power. In the bilayer structures, the thickness of the second layer is much thicker than that of the first layer. The measured optical properties are mainly influenced by the second layer. Therefore, these results suggest that higher RF power leads to the lower optical bandgap. These results are in good agreement with our previous report.[22] In addition, the optical bandgap slightly increased after the post-deposition annealing, suggesting that non-bonded hydrogen in as-deposited film was rearranged during the annealing process. The effective lifetime for the as-deposited samples was very low (5–7 μs); however, the post-deposition annealing drastically improved the effective lifetime. The effective lifetime increased

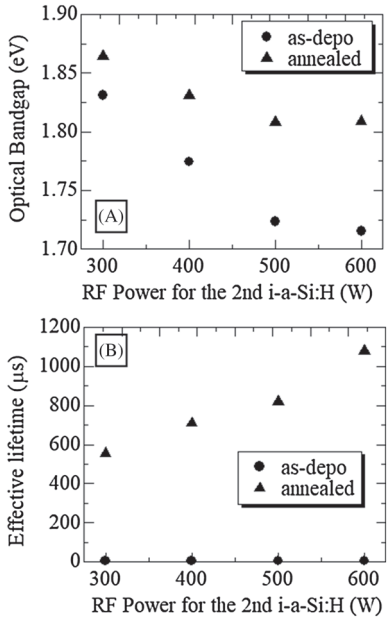

FIGURE 3 Dependence of (A) optical bandgap and (B) τ_{eff} on the RF power for the second i-a-Si:H sputtering. The RF power for the first i-a-Si:H was fixed at 300 W. The optical bandgap was estimated from spectroscopic ellipsometry analyses using Tauc–Lorentz model. The value of τ_{eff} corresponds to the minority carrier density of 10^{15} cm^{-3}. The post-deposition annealing temperatures were 300°C–350°C

with increasing the RF-power and exceeded 1 ms at the RF power of 600 W. In our previous work using single FTS-deposited i-a-Si:H passivation layer, the increase of the RF-power led to the deterioration of the effective lifetime. Our previous report also pointed out that the photoconductivity of i-a-Si:H deposited on a glass substrate increased with increasing the RF-power. These previous findings suggest that high RF power sputtering leads to the improvement of i-a-Si:H quality and large sputtering damage to the c-Si surface simultaneously. As shown in Figure 3B, the i-a-Si:H deposited at high RF-power shows better passivation quality. This clearly indicates that the first i-a-Si:H layer deposited at low RF power effectively suppressed the sputtering damage to the surface of c-Si.

Figure 4 shows the effect of the RF power for the first i-a-Si:H deposition on optical bandgap and effective lifetime. The optical bandgap decreased with increasing the RF power as well as the first experiment as shown in Figure 3. The influence of the RF-power for the first i-a-Si:H deposition on the optical bandgap was weaker than that for the second i-a-Si:H deposition due to the thickness difference (the first i-a-Si:H layer: 1 nm, the second i-a-Si:H layer: 5 nm). The highest effective lifetime was obtained at an RF power of 300 W. Higher or lower RF power leads to the deterioration of the passivation quality. The deterioration of the passivation quality for RF power higher than 300 W can be explained by sputtering damage to the c-Si wafer. The deterioration of the passivation quality for RF power lower than 300 W is due to the very poor quality of i-a-Si:H as reported in our previous work.[22]

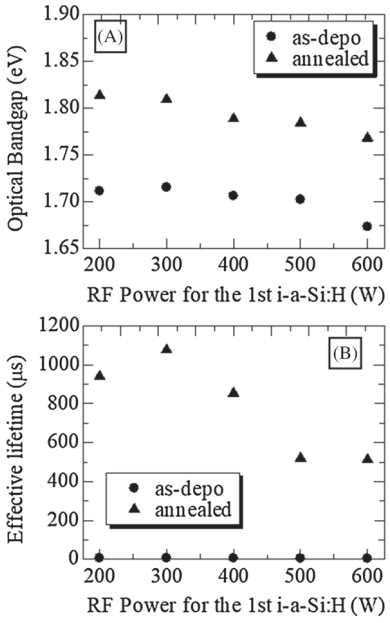

FIGURE 4 Dependence of (A) optical bandgap and (B) τ_{eff} on the RF power for the first i-a-Si:H sputtering. The RF power for the second i-a-Si:H was fixed at 600 W. The optical bandgap was estimated from spectroscopic ellipsometry analyses using Tauc–Lorentz model. The value of τ_{eff} corresponds to the minority carrier density of 10^{15} cm^{-3}. The post-deposition annealing temperatures were 300°C–350°C

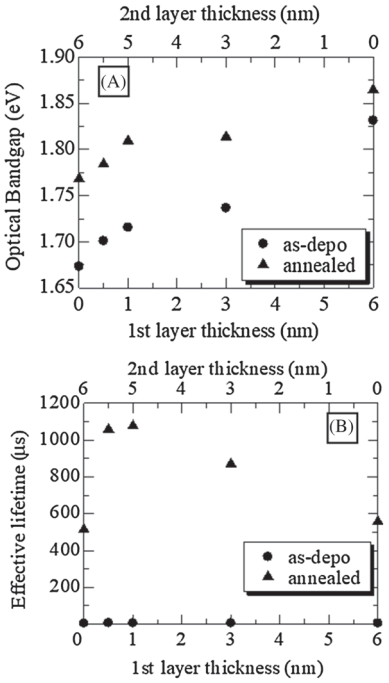

FIGURE 5 Dependence of (A) optical bandgap and (B) τ_{eff} on the thickness of the first i-a-Si:H layer. The total thickness of the i-a-Si:H layer was fixed at 6 nm. The RF powers for the first and second i-a-Si:H were fixed at 300 and 600 W, respectively. The optical bandgap was estimated from spectroscopic ellipsometry analyses using Tauc–Lorentz model. The value of τ_{eff} corresponds to the minority carrier density of 10^{15} cm^{-3}. The post-deposition annealing temperatures were 300°C–350°C

Figure 5 shows the effect of the first i-a-Si:H layer thickness on optical bandgap and effective lifetime. In this experiment, the optimum RF power condition (first layer deposition: 300 W, second layer deposition: 600 W) was employed. As predicted from the previous results, the optical bandgap increased by increasing the thickness of the first i-a-Si:H layer because i-a-Si:H deposited at low RF power shows a higher optical bandgap. The effective lifetime drastically increased by inserting the first i-a-Si:H layer. This is due to the suppression of sputtering damage as mentioned above. The effective lifetimes were almost similar when the thickness of the first i-a-Si:H layer was 0.5 nm and 1.0 nm, proving that the sputtering damage can be suppressed by using 0.5-nm-thick i-a-Si:H deposited at an RF-power of 300 W. These results clearly indicate that the suppression of the sputtering damage (insertion of i-a-Si:H deposited at low RF power) and the use of high quality i-a-Si:H (high RF-power deposition) are the key factors to achieve good surface passivation.

Finally, we slightly modified the DC power for further improvement of passivation quality. In this experiment, the DC power of 56 W was employed. Figure 6 shows the dependence of carrier lifetime on minority carrier density of the c-Si wafer passivated with i-a-Si:H deposited by DC-superimposed RF-FTS using two-step deposition method. The result for the c-Si passivated with i-a-Si:H deposited by one-step deposition is also shown for comparison. The i-a-Si:H deposited using the two-step deposition method shows a higher effective lifetime for through the entire minority carrier density range. An effective lifetime of 1.38 ms at a minority carrier density of 10^{15} cm^{-3} was achieved. The corresponding i*V*oc at one sun was

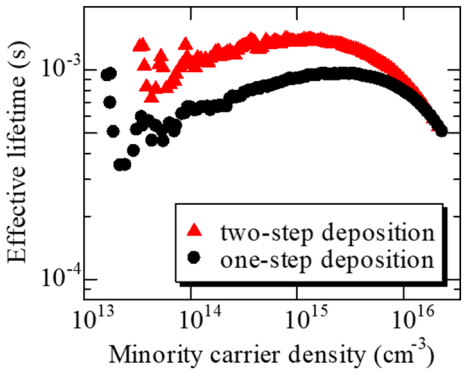

FIGURE 6 Dependence of τ_{eff} on the minority carrier density. The total thickness of i-a-Si:H was 5 nm. The first and second layer thicknesses were 0.5 and 4.5 nm, respectively. The first layer was deposited at a radio frequency (RF) power of 300 W. The second layer was deposited at an RF power of 600 W. For the one-step deposition, the RF power was 300 W. The DC power was fixed at 56 W for both cases [Colour figure can be viewed at wileyonlinelibrary.com]

0.701 V. The average deposition rate during the two-step deposition method was 14.1 nm/min. In addition, we also fabricated a SHJ solar cell with this i-a-Si:H layer deposited by DC-superimposed RF-FTS using the two-step deposition method. Figure 7A shows the illuminated current density–voltage (*J*-*V*) curve of the fabricated SHJ solar

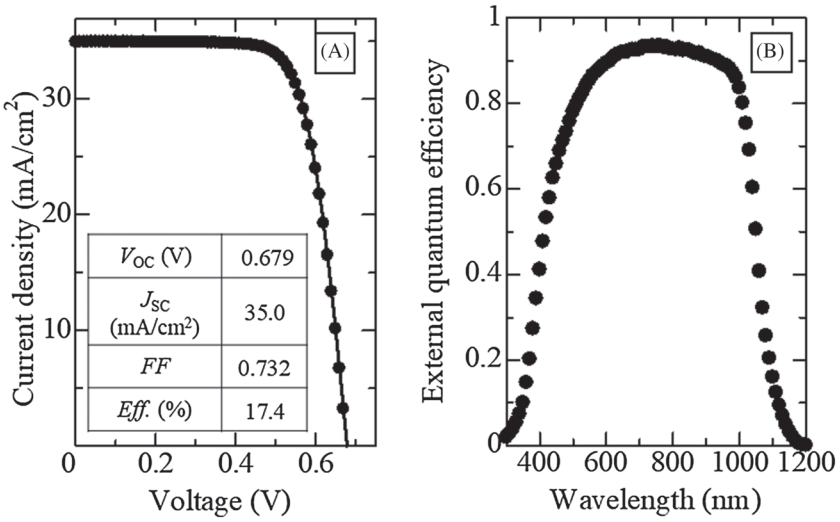

FIGURE 7 (A) *J-V* curve of the SHJ solar cell with i-a-Si:H passivation layers deposited by DC-superimposed RF-FTS using two-step deposition method under AM1.5 illumination and (B) External quantum efficiency of the SHJ solar cell

cell. The external quantum efficiency is also shown in Figure 7B. The SHJ solar cell showed a relatively high J_{SC} although a non-textured c-Si wafer was used.[26] This is due to the double anti-reflection effect of the LiF and ITO layers on the front side of the SHJ solar cell.[27] Without the LiF anti-reflection layer, the J_{SC} was 34.1 mA/cm^2. The solar cell showed an open circuit voltage (Voc) of 0.679 V. This value is slightly lower than the *i*Voc measured from the lifetime sample (i-a-Si:H (two-step deposition, 5 nm)/n-type c-Si (280 μm)/i-a-Si:H (two-step deposition, 5 nm)). We also measured the effective lifetime of an n-type hydrogenated microcrystalline silicon (30 nm) /i-a-Si:H (2.5 nm)/n-type c-Si (280 μm)/i-a-Si:H (2.5 nm)/n-type hydrogenated microcrystalline silicon (30 nm) structure to assess the rear side passivation quality. This sample showed an *i*Voc of 0.722 V (minority carrier lifetime of 5.4 ms at a carrier density of 10^{15} cm^{-3}). This indicates that the rear side passivation quality is not the reason for the *V*oc limitation. We have found that the deterioration of the *i*Voc occurs after the deposition of the p-type layer. The *i*Voc of the solar cell precursor with the structure of p-type hydrogenated microcrystalline silicon oxide (20 nm) /i-a-Si:H (2.5 nm)/n-type c-Si (280 μm)/i-a-Si:H (2.5 nm)/n-type hydrogenated microcrystalline silicon (30 nm) was 0.683 V. Therefore, it is important to optimize the p-type layer for further improvement of the *V*oc. Although the V_{OC} of the SHJ solar cell with i-a-Si:H deposited by DC-superimposed RF-FTS using the two-step deposition method is lower than that of the SHJ solar cell with i-a-Si:H deposited by PECVD, our solar cell performance is the best result for SHJ solar cells with i-a-Si:H deposited by a sputtering method.

4 | CONCLUSIONS

The two-step deposition method is a promising technique to improve the c-Si surface passivation quality of i-a-Si:H deposited by facing target sputtering. The first i-a-Si:H deposited at low RF power effectively suppresses the sputtering damage during the deposition of the second i-a-Si:H at high RF power. Only 0.5-nm-thick first i-a-Si:H layer is enough to prevent the sputtering damage to the c-Si wafer. Under the optimized condition, the c-Si wafer passivated with 5-nm-thick i-a-Si:H showed an effective lifetime of 1.38 ms (*i*Voc at one sun: 0.701 V). This promising passivation layer can be deposited at a deposition rate of 14.1 nm/min without substrate heating.

ACKNOWLEDGEMENT

This work was supported by New Energy and Industrial Technology Development Organization (NEDO; 15100647-0).

ORCID

Yuta Shiratori https://orcid.org/0000-0001-8074-455X
Kazuyoshi Nakada https://orcid.org/0000-0002-2219-6345
Shinsuke Miyajima https://orcid.org/0000-0002-0184-3152

REFERENCES

1. Blakers AW, Wang A, Milne AM, Zhao J, Green MA. 22.8% efficient silicon solar cell. *Appl. Phys. Lett.* 1989;55:1363-1365. https://doi.org/10.1063/1.101596
2. Schmidt J, Merkle A, Brendel R, Hoex B, de Sanden MV, Kessels WM. Surface passivation of high-efficiency silicon solar cells by atomic-layer-deposited Al2O3. *Prog Photovoltaics Res Appl*. 2008;16(6):461-466. https://doi.org/10.1002/pip.823
3. Min B, Müller M, Wagner H, et al. A roadmap toward 24% efficient PERC solar cells in industrial mass production. *IEEE J Photovoltaics*. 2017;7(6):1541-1550. https://doi.org/10.1109/JPHOTOV.2017.2749007
4. Masuko K, Shigematsu M, Hashiguchi T, et al. Achievement of more than 25% conversion efficiency with crystalline silicon heterojunction solar cell. *IEEE J. Photovoltaics*. 2014;4(6):1433-1435.
5. Adachi D, Hernández JL, Yamamoto K. Impact of carrier recombination on fill factor for large area heterojunction crystalline silicon solar cell with 25.1% efficiency. *Appl. Phys. Lett.* 2015;107:22-25. https://doi.org/10.1063/1.4937224
6. Yoshikawa K, Kawasaki H, Yoshida W, et al. Silicon heterojunction solar cell with interdigitated back contacts for a photoconversion efficiency over 26%. *Nature Energy*. 2017;2(5):17032. https://doi.org/10.1038/nenergy.2017.32

7. De Wolf S, Descoeudres A, Holman ZC, Ballif C. High-efficiency silicon heterojunction solar cells: a review. *Green*. 2012;2(0):7-24. https://doi.org/10.1515/green-2011-0039
8. Liu W, Zhang L, Chen R, at al. Underdense a-Si:H film capped by a dense film as the passivation layer of a silicon heterojunction solar cell. *J Appl Phys*. 2016;120(17):175301. https://doi.org/10.1063/1.4966941
9. Sai H, Chen P, Hsu H, Matsui T, Nunomura S, Matsubara K. Impact of intrinsic amorphous silicon bilayers in silicon heterojunction solar cells. *J Appl Phys*. 2018;124(10):103102. https://doi.org/10.1063/1.5045155
10. Louwen A, van Sark WG, Schropp RE, Turkenburg WC, Faaij AP, Cost analysis of two silicon heterojunction solar cell designs, 2013 IEEE 39th Photovolt. Spec. Conf. (2013) 3357–3361. https://doi.org/10.1109/PVSC.2013.6745170
11. Naoe M, Yamanaka S, Hoshi Y. Facing targets type of sputtering method for deposition of magnetic metal films at low temperature and high rate. *IEEE Trans Magn*. 1980;MAG-16:646–648. https://doi.org/10.1109/TMAG.1980.1060683
12. Hoshi Y, Kato HO, Funatsu K. Structure and electrical properties of ITO thin films deposited at high rate by facing target sputtering. *Thin Solid Films*. 2003;445(2):245-250. https://doi.org/10.1016/S0040-6090(03)01182-9
13. Hoshi Y, Kobayashi SI, Uchida T, Sawada Y, Lei H. Development of low damage sputter-deposition method for the preparation of organic light emitting diode. *J Vac Soc Japan (in Japanese)*. 2016;59:59-64.
14. Yu W, Meng LH, Yuan J, Lu HJ, Wu SJ, Fu GS. Influence of substrate temperature on growth of a-Si:H films by reactive facing target sputtering deposition. *Science China Physics, Mechanics and Astronomy*. 2010;53(5):807–811. https://doi.org/10.1007/s11433-010-0193-z
15. Descoeudres A, Barraud L, De Wolf Stefaan SB, at al. Improved amorphous/crystalline silicon interface passivation by hydrogen plasma treatment. *Appl Phys Lett*. 2011;99(12):123506. https://doi.org/10.1063/1.3641899
16. Koyama K, Ohdaira K, Matsumura H. Extremely low surface recombination velocities on crystalline silicon wafers realized by catalytic chemical vapor deposited SiNx/a-Si stacked passivation layers. *Appl. Phys. Lett*. 2010;97:82108. https://doi.org/10.1063/1.3483853
17. Nakada K, Miyajima S, Konagai M, Amorphous silicon oxide passivation films for silicon heterojunction solar cells studied by hydrogen evolution, *Jpn. J. Appl. Phys*. 2014;53:04ER13. doi:https://doi.org/10.7567/JJAP.53.04ER13
18. Zhang H, Nakada K, Miyajima S, Konagai M. High-performance a-Si1-xOx:H/c-Si heterojunction solar cells realized by the a-Si:H/a-Si1-xOx:H stack buffer layer. *Phys Status Solidi RRL*. 2015;9(4):225-229. https://doi.org/10.1002/pssr.201409546
19. Tsuzaki S, Ohdaira K, Oikawa T, Koyama K, Matsumura H. Improvement in passivation quality and open-circuit voltage in silicon heterojunction solar cells by the catalytic doping of phosphorus atoms. *Jpn. J. Appl. Phys*. 2015;54:072301. https://doi.org/10.7567/JJAP.54.072301
20. Zhang X, Hargreaves S, Wan Y, Cuevas A. Surface passivation of crystalline silicon by sputter deposited hydrogenated amorphous silicon. *Phys Status Solidi – Rapid Res Lett*. 2014;8(3):231-234. https://doi.org/10.1002/pssr.201308253
21. Zhang X, Cuevas A, Demaurex B, De Wolf S. Sputtered hydrogenated amorphous silicon for silicon heterojunction solar cell fabrication. *Energy Procedia*. 2014;55:865-872. https://doi.org/10.1016/j.egypro.2014.08.070
22. Shiratori Y, Zulkifly FA, Nakada K, Miyajima S. Effect of RF power on the properties of intrinsic hydrogenated amorphous silicon passivation layer deposited by facing target sputtering. *Appl Phys Express*. 2018;11(3):31301. https://doi.org/10.7567/APEX.11.031301
23. Shiratori, Y., Kim, J., Nakada, K. and Miyajima, S., Silicon heterojunction solar cell with intrinsic hydrogenated amorphous silicon layer deposited by facing target sputtering, 2018 IEEE 7th World Conf. Photovolt. Energy Conversion, WCPEC 2018 - A Jt. Conf. 45th IEEE PVSC, 28th PVSEC 34th EU PVSEC. (2018) 3142–3147. doi:https://doi.org/10.1109/PVSC.2018.8547972
24. Jellison GE Jr, Modine FA. Parameterization of the optical functions of amorphous materials in the interband region. *Appl Phys Lett*. 1996;69(3):371-373. http://link.aip.org/link/?APL/69/371/1
25. Shiratori Y, Nakada K, Miyajima S. Effect of superimposed DC power on the properties of intrinsic hydrogenated amorphous silicon passivation layer deposited by RF facing target sputtering. *IEEE J. Photovoltaics*. 2020. https://doi.org/10.1109/jphotov.2020.2989174
26. Kim J, Takiguchi Y, Nakada K, Miyajima S, Silicon heterojunction solar cells with Cu2O:N as p-type layer, 2018 IEEE 7th World Conf. Photovolt. Energy Convers. (A Jt. Conf. 45th IEEE PVSC, 28th PVSEC 34th EU PVSEC). (2018) 2145–2150.
27. Ateto EO, Konagai M, Miyajima S. Triple layer antireflection design concept for the front side of c-Si heterojunction solar cell based on the antireflective effect of nc-3C-SiC:H emitter layer. *Int J Photoenergy*. 2016;2016:5282851hyphen;5282859. https://doi.org/10.1155/2016/5282851

How to cite this article: Bin Mohd Zulkifly FA, Shiratori Y, Nakada K, Miyajima S. Impact of bilayer structures on the surface passivation quality of high-rate-sputtered hydrogenated amorphous silicon for silicon heterojunction solar cells. *Prog Photovolt Res Appl*. 2020;28:971–976. https://doi.org/10.1002/pip.3298